DOI: 10.61782/fa.2025.0099

ACTIVE STRUCTURAL ACOUSTIC CONTROL WITH REMOTE MICROPHONE TECHNIQUE FOR NOISE RADIATED BY A THIN PLATE

Francesco Mori[1*] **Andrea Santoni**[1] **Cristina Marescotti**[1]
Patrizio Fausti[1] **Francesco Pompoli**[1] **Pietro Nataletti**[2] **Paolo Bonfiglio**[3]
[1] Department of Engineering, University of Ferrara, Italy
[2] INAIL, National Institute for Insurance against Accidents at Work, Rome, Italy
[3] Materiacustica srl, Via C. Ravera 15/A, Ferrara, Italy

ABSTRACT

Noise pollution in industrial environments can significantly impact workers' health and productivity, necessitating effective control measures. This preliminary study investigates the feasibility of an active structural acoustic control (ASAC) system to mitigate noise radiated by an industrial cabin wall. A cabin mock-up was created for this purpose, designed with passive acoustic treatments to improve noise insulation on three walls, the floor and the roof. Conversely, one of the cabin walls was realized with a thin steel plate without passive acoustic treatments. The ASAC system, applied to this plate, uses a single inertial actuator to suppress noise induced by an acoustic source inside the cabin and radiated to the external environment. The system employs the remote microphone technique (RMT) to attenuate the noise at a specific distance from the cabin. The experimental validation was conducted for different types of disturbing noise signals. The results highlight the potentiality of this method to control radiated noise. This work lays the foundation for scalable ASAC solutions in industrial environments, offering a promising path toward quieter workplaces.

Keywords: *industrial cabin, active structural acoustic control, FXLMS algorithm, remote microphone technique*

[*] ***Corresponding author***: francesco.mori@unife.it.

1. INTRODUCTION

In industrial environments, enclosures are commonly used to reduce airborne noise propagation and workers' exposure. These structures typically consist of a mass-spring-mass system, with an outer continuous plate, an inner perforated plate inside and a fibrous material in between, acting as both a spring of the system and noise absorber. However, these enclosures can often have untreated parts, such as panels and windows, reducing the overall effectiveness. In such cases, an active structural acoustic control (ASAC) system can help mitigate low-frequency noise radiation toward the external environment. An ASAC system employs one or more actuators on a vibrating surface to generate an anti-vibration signal that counteracts noise radiation. This signal is computed in real-time through an adaptive algorithm after the acquisition of some signals from error and reference sensors, similarly to an active noise control (ANC) system. Literature discourages the use of accelerometers as error sensors due to the need of multiple sensors and actuators [1]. Several studies explored the optimization of number and placement of actuators on radiating surfaces [2]. However, practical industrial applications [3] remain limited compared to numerical studies and laboratory experiments.
This study, part of the BRIC Inail 2022 ID-11 project, investigates the feasibility of applying an ASAC system to an industrial cabin mock-up. The system was applied on a thin steel plate representing one cabin wall, radiating noise generated by a simulated source enclosed in the cabin and emitting different types of signals. The system operates in a feedforward configuration with one reference microphone inside the cabin, one inertial actuator on the radiating plate and one error microphone near the outer plate. Additionally, a remote microphone technique (RMT) was employed for

far-field noise attenuation [4] and feedback compensation was used to prevent reference signal corruption [5]. The implemented adaptive algorithm was the filtered-X least mean squares (FXLMS) [6], chosen for its simple scalability for further developments. Section 2 provides an overview of the case study, detailing the ASAC system design and the implemented algorithm. Section 3 presents the study findings, including the preliminary characterization of the impulse responses and the attenuation obtained for different noise signals. Finally, Section 4 outlines the conclusions and potential future developments to enhance the system performance.

2. EXPERIMENTAL SETUP AND ASAC SYSTEM

The tests were conducted on the reproduction of an industrial enclosure, as shown in Fig. 1. The structure measures 1.5 × 1.5 × 2.0 m and features a 1 mm-thick steel plate on one side. The remaining walls and the roof are made of similar steel plates, internally treated with sound-absorbing fibrous material and a metallic mesh. Conversely, the floor features a 5 mm-thick steel plate instead of the metallic mesh. Inside the enclosure, an acoustic dodecahedron reproduces synthetized signals and recordings of industrial machineries as a simulated noise source.

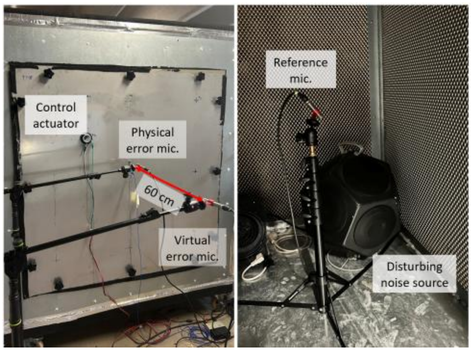

Figure 1. Experimental setup outside and inside the enclosure.

The ASAC system was implemented on the steel plate in a feedforward configuration. The reference microphone was placed inside the cabin, near the noise source. The inertial actuator, generating the control signal, was selected based on the frequency response comparison of several actuators and placed on the plate away from the edges, where distortions were observed in some preliminary tests probably related to the boundary rigidity. The system adopts the remote microphone technique (RMT), which virtualizes the error microphone position to prevent a physical obstacle during the real application [4]. In this setup, the physical error microphone was placed outside, near the steel plate, while the virtual error microphone was positioned 60 cm from the surface. The entire ASAC system is driven by a NI cRIO 9063 real-time target, acquiring and generating signals at a 3200 Hz sampling rate. Due to this rate and device placement, the system does not meet the causality constraint, making it ineffective for unpredictable signals. The algorithm employed to compute the adaptive filter was the feedforward filtered-X least mean squares with acoustic feedback compensation (FF_FBFXLMS) [5], chosen to prevent reference signal corruption caused by plate excitation.

The whole procedure executed by the ASAC system is hereinafter described. In a preliminary stage, the virtual and physical secondary paths (s_v and s_p respectively) and the feedback path (f) are estimated generating a white noise with the control source and computing the filter with a least mean square (LMS) approach [6]. Similarly, the virtual and physical primary paths (p_v and p_p) are estimated emitting white noise with the disturbing source. The impulse response h_{pv} between the physical and the virtual positions can be derived from the ratio of the two primary paths in the frequency domain. After this stage, the virtual error microphone is no longer involved in the ASAC operations and assumes a simple monitoring function. During the online operations, the ASAC system works iteratively as follows:

- the reference signal $u(n)$ is acquired and the contribution from the control actuator is subtracted:

$$x(n) = u(n) - f * y(n), \tag{1}$$

  where $y(n)$ is the output of the control source and $*$ is the convolutional operator.
- The disturbing signal in the physical position is computed from the physical error signal $e_p(n)$ as:

$$d_p(n) = e_p(n) - s_p * y(n). \tag{2}$$

- The virtual error signal $e_v(n)$ is evaluated as:

$$e_v(n) = h_{pv} * d_p(n) + s_v * y(n). \tag{3}$$

- The FXLMS computes the adaptive filter and drives the inertial actuator with the classical procedure, using the virtual error signal $e_v(n)$ and the cleaned reference signal $x(n)$ as inputs.

3. RESULTS

3.1 Estimation of the impulse responses

The secondary and primary paths, used for the identification of the system impulse responses, are illustrated in Fig. 2 and Fig. 3, respectively, for both the physical and the virtual positions. These functions are shown in terms of transfer function magnitude in the frequency domain for easier interpretation. As can be observed, the secondary paths exhibit higher amplitude than the primary paths across the entire spectrum. This means that for equal power of the sources, actuator saturation can be avoided. The amplitude at the virtual position is lower than at the physical position due to the larger distance from the radiating surface. Fig. 4 shows the feedback path. The contribution of the control actuator on the reference microphone is particularly relevant at low frequency (< 50 Hz). However, its importance depends on the noise level produced by the disturbing source. A filter length of 2000 elements was assumed for primary, secondary and feedback paths.

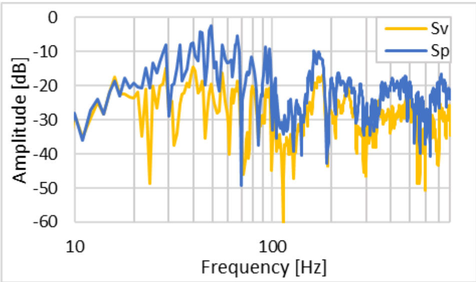

Figure 2. Physical and virtual secondary paths.

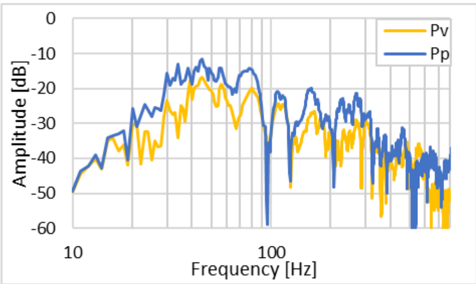

Figure 3. Physical and virtual primary paths.

The transfer function H_{pv} (with a capital letter to indicate the frequency domain) used to model the disturbance signal at the virtual position, is reported in Fig. 5. This function was obtained as the ratio between the spectra of the virtual and the physical primary paths. A positive value means that the sound pressure level at the virtual position assumes a larger value with respect to the physical position for that frequency. It should be noted that this function models the acoustic field at the virtual position starting from the sensing of the acoustic field in one point near the radiating plate. However, the noise at the virtual position can be radiated from different points of the plate. Thus, this function considers only a part of the disturbing noise. A filter length of 500 elements was considered for the physical-virtual impulse response.

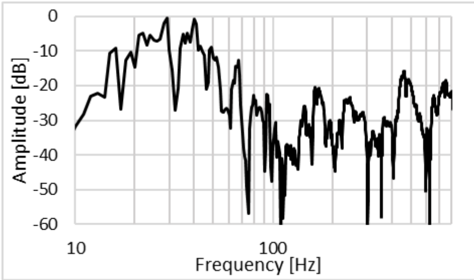

Figure 4. Feedback path.

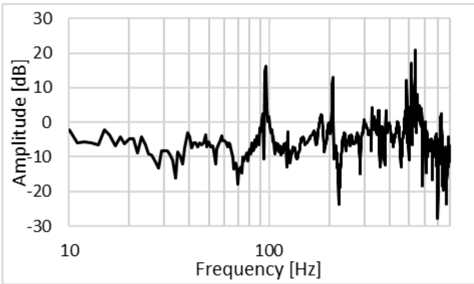

Figure 5. Physical-virtual transfer functions.

3.2 Attenuation of noises

The results obtained with different pure tones are shown in Tab. 1. These frequencies were selected as the central frequencies of the third octave bands within the range of interest, independently of the plate modal frequencies.
The ASAC system successfully attenuates noise at the virtual position for all the tones, except for the 125 Hz frequency, where a slight amplification occurs. This particular tone is characterized by a low level on the primary paths. Thus, the estimation of H_{pv} at that frequency can be not accurate. The 160 Hz tone coincides with a

radiating mode, as indicated by the peaks in the primary and secondary path spectra.
Secondly, a pseudo-random noise signal was used for the performance evaluation. This signal contains a broad frequency range but maintains a periodic pattern, repeating every 0.2 s. The results for this signal are shown in Fig. 6. In this case, the ASAC system faces more difficulties in providing a good performance, although noise attenuation is observed across all the bands of interest. This results in an overall noise attenuation of 1.6 dB – 1.9 dB(A).
Finally, Fig. 7 shows the effect of the ASAC system on the noise generated by an industrial compressor. The system reduces noise across the bands from 80 Hz to 500 Hz, especially on the main components at 80 Hz and 200 Hz, achieving an overall attenuation of 3.5 dB – 2.9 dB(A).

Table 1. Attenuation for different pure tones.

Frequency [Hz]	125	160	200	250	315	400
Attenuation [dB]	-2.3	4.8	3.9	7.0	13.6	2.4

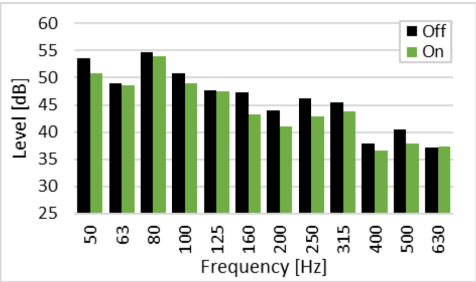

Figure 6. Results for a pseudo-random noise signal.

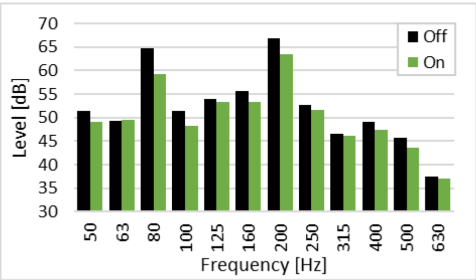

Figure 7. Results for an industrial compressor recording.

4. CONCLUSIONS

In this paper, an experimental study on the potentiality of a feedforward ASAC system with RMT and feedback compensation was analyzed. The results show that the ASAC system can act on all the components in the frequency range of interest, when the physical-virtual impulse response in effectively modelled. No tests with pure broadband signals were carried out, since the causality constraint was not respected. However, the ASAC system was effective in the cases of a pseudo-random noise signal and industrial compressor recording. The possible future steps of this study could regard the optimization of number and placement of error microphones and actuators, for extending the zone of quiet at the virtual position. Furthermore, tests with actuators applied to the treated panels could be explored.

5. ACKNOWLEDGMENTS

This work was supported by the BRiC 2022 ID-11 project from INAIL (National Institute for Insurance against Accidents at Work).

6. REFERENCES

[1] V.L. Metcalf, C.R. Fuller, R.J. Silcox, and D.E. Brown: "Active control of sound transmission/radiation from elastic plates by vibration inputs, II: Experiments", *J. Sound Vib.*, Vol. 153, no. 3, pp. 387-402, 1992.

[2] S. Wrona, and M. Pawelczyk: "Experimental investigation on inertial actuators arrangement optimization for active control applications", in *Proc. of Forum Acusticum 2023,* (Turin, Italy), 2023.

[3] S. Wrona: "Performance analysis of active structural acoustic control applied to a washing machine", *Sensors*, Vol. 22, no. 7357, 2022.

[4] J. Cheer, and S. Daley: "Active structural acoustic control using the remote sensor method", *J. Phys.: Conf. Ser.*, Vol. 744, no. 012184, 2016.

[5] F. Mori, A. Santoni, P. Fausti, F. Pompoli, P. Bonfiglio, and P. Nataletti: "The effectiveness of least mean squared-based adaptive algorithms for active noise control system in a small confined space", *App. Sci.*, Vol. 13, no. 11173, 2023.

[6] S.M. Kuo, I. Panahi, K.M. Chung, T. Horner, M. Nadeski, and J. Chyan: *Design of active noise control systems with the TMS320 family*, Texas Instruments, 1996.